Journal of Molecular Structure 1091 (2015) 125–132

Contents lists available at ScienceDirect

Journal of Molecular Structure

journal homepage: www.elsevier.com/locate/molstruc

Unravelling the reaction mechanism of matrix metalloproteinase 3 using QM/MM calculations

Gustavo Troiano Feliciano [a,*], Antônio José Roque da Silva [b,c]

[a] Departamento de Físico-química, Instituto de Química, Universidade Estadual Paulista Júlio de Mesquita Filho (UNESP), Rua Prof. Francisco Degni 55, 14800-900 Araraquara, São Paulo, Brazil
[b] Instituto de Física de Universidade de São Paulo (USP), CP 66318, 05315-970 São Paulo, SP, Brazil
[c] Laboratório Nacional de Luz Síncrotron (LNLS), CP 6192, 13083-970 Campinas, SP, Brazil

HIGHLIGHTS

- MMP3 enzyme reaction mechanism is studied by QM/MM DFT simulation techniques.
- Reactant structure always displays a tetrahedrally coordinated zinc atom.
- The calculations support the acid–base catalyzed pathway for the MMP3 enzyme.
- Partial detachment of one histidine residue from zinc in reactant state is observed.
- The reaction is concerted, with a computed barrier of 14.8 kcal/mol.

ARTICLE INFO

Article history:
Received 18 September 2014
Received in revised form 2 February 2015
Accepted 25 February 2015
Available online 5 March 2015

Keywords:
Matrix metalloproteins
Enzyme catalysis
QMMM

ABSTRACT

The matrix metalloproteinase family (MMP) constitutes a family of zinc (Zn) proteases that catalyze the breaking of peptide bonds in proteins. These enzymes are very promising drug targets, since they are involved in remodeling and degradation of the extracellular matrix, which is a key process required for cancer metastasis, and thus, their reaction mechanism has been an area of intensive research. Early proposal based on acid base catalyzed hydrolysis, suggested that a conserved zinc bound water molecule acted as the nucleophile attacking the peptide bond carbon, after being activated by essential glutamate. The possibility of a direct nucleophilic attack by the enzyme, performed by the glutamate was also suggested. These are the key yet unsolved issues about MMP reaction mechanism.

In the present work, we used hybrid quantum/classical calculations to analyze the structure and energetics of different possible hydrolysis reaction paths. The results support a water mediated mechanism, where both the nucleophile water molecule and the carbonyl oxygen of the scissile peptide bond are coordinated to zinc in the reactive configuration, while the essential glutamate acts as the base accepting the proton from the nucleophilic water. Formation of the carbon–oxygen bond and breaking of carbon–nitrogen bond were found to be concerted events, with a computed barrier of 14.8 kcal/mol. Substrate polarization was found to be important for the observed reaction mechanism, and a substantial change in the metal coordination environment was observed, particularly, regarding the zinc–histidine coordination.

Introduction

The matrix metalloproteinase (MMP) family of zinc (Zn) proteases is involved in the homeostatic regulation of the extracellular environment and in innate immunity. These enzymes make use of an endogenously coordinated zinc (2+) atom, in order to hydrolyze peptide bonds. Abnormal MMP function has implications in diseases such as cancer, arthritis, stroke and atherosclerosis. Therefore, they have been a pharmaceutical target for over 20 years [1–5]. Despite massive research, only one MMP inhibitor (Periostat) has been approved by the FDA. Possible reasons for low success rate of MMP inhibitors are the unwanted side effects due to their lack of selectivity. The MMP family includes more than 28 different proteins, with several domain architectures. The catalytic domains can be classified as: GPI, S anchored which includes MMP 11, 17 and MMP25; Transmembrane MMPs include MMP14, MMP15, MMP24 and MMP16 Ifs 1 and 2; Non-furin regulated

* Corresponding author.

http://dx.doi.org/10.1016/j.molstruc.2015.02.079
0022-2860/

MMPs, MMPs 1, 3, 7, 8, 10, 12, 13, 20 and 27; The so called gelatinases, MMP2 and MMP9; other MMPs 19 IF1 and IF6, 21, 23 A and B, 26 and 28 IF1 and 2. The typical domain architecture of MMPs consists of the Catalytic Domain (CD)+ N terminal prodomain (pro)+ C terminal Hemopexin like domain (HPX). Additionally both gelatinases have three Fibronectin repeats (FN) intercalated in the CD. Interestingly in both cases the CD can stand alone and function as MMP [6]. X-ray structures are available for several MMP CDs, including some MMP-inhibitor complexes. MMPs 1, 2, 3 and 9 have been also determined with the Pro domain. All CD structures show the presence of 1 or 2 zinc ions. In the case of 2 zinc ions, usually one zinc atom has a structural function, while the other has the catalytic function. The structures also reveal the presence of up to three calcium ions. The structural zinc is tetrahedrally coordinated with three histidine residues and one aspartic acid residue, while the catalytic zinc is coordinated with three histidine residues and a cystein residue, in the inactive pro-form. In the activation process, MMP is cleaved and the pro domain containing the coordinating cysteine is released, and the substrate gains access to the catalytic zinc atom [7]. The precise coordination structure of catalytic zinc is still under debate and directly related to the mechanism studied in the present work (see below). For example, structures of the active MMPs show that the active zinc atom could be coordinated with one to three water molecules (or possibly hydroxide anions), in addition to the conserved histidine residues [8–10].

Among the zinc metalloproteases, MMPs have some unique features: (i) the coordination sphere around zinc, which is usually composed of two histidine and one glutamate residues, as in thermolysin and carboxypeptidase, is instead composed of three histidine residues in the MMPs as previously described, and (ii) the absence of a basic residue (usually arginine) around the carbonyl group of the scissile peptide bond of the substrate, like in common zinc proteases [8]. These features have important implications for the reaction mechanism, and also make the MMPs differentiated drug targets.

The proposed reaction mechanisms for MMP follow that for other related zinc-peptidases and are depicted in Fig. 1: (i) a water-mediated nucleophilic attack, into which a conserved glutamate side chain in the active site performs acid–base catalysis, removing one proton from the attacking water and subsequently donating it to the nitrogen of the cleaved peptide bond. These two steps can be in principle, stepwise or concerted; (ii) a glutamate-mediated nucleophilic attack, into which the carboxylic group of the conserved glutamate attacks the peptide bond directly, giving rise to an anhydride acyl-enzyme intermediate, and in a second step, an incoming water molecule attacks the intermediate to free the products and regenerate the initial state of the enzyme.

There is evidence favoring both mechanisms, mainly for other related zinc metalloproteases, like thermolysin and carboxypeptidase-A (CPA). Evidence for the water-attack mechanism was obtained for CPA, by means of X-ray diffraction experiments [11] and by ^{18}O isotopic labeling [12], which demonstrated that the acyl-enzyme intermediate generation is unlikely, in the hydrolysis of peptide substrates, but it would be feasible for other non-natural ester substrates. However, evidence for the glutamate-mediated attack is also derived from studies of CPA, being historically the first to enzyme where the mixed tetrahedral anhydride intermediate was observed using spin-labeling and ENDOR resonance techniques [13]. In other work, it was observed that CPA can display a stable enzyme-bound acyl intermediate in studies using Gly-Tyr dipeptide as substrate, and the intermediate hydrolysis is the rate-limiting step [14].

Theoretical methods constitute a powerful and invaluable tool for the study of enzyme reaction mechanism. In this context, the Quantum Mechanics/Molecular Mechanics (QM/MM) methods developed in the last decades are the best choice. In this methodology, the system is partitioned in two regions (i) the reactive region described by Quantum Mechanics (QM), where chemical bonds are effectively rearranged, and so, an electronic description is necessary, and (ii) the environment or classical regions described by classical (i.e. MM) force fields, parameterized by an empirical potential, enough to represent the environment (the protein structure and the solvent). CPA and thermolysin have already been studied with QM/MM methods, showing that with the natural substrate of relatively small barrier of 14.6 kcal/mol barrier is found for the water-mediated attack [15]. In another DFT-B3LYP ONIOM study of the MMP3 enzyme [16], a single step reaction consisting of a water nucleophilic attack with a barrier of 13.1 kcal/mol was predicted, with acetamide as the model substrate. More recent studies of the reaction catalyzed by MMP-2 with its natural substrate [17], pointed out to the flexibility of the substrate as an important element during the reaction. Concerning the anhydride mechanism, molecular dynamics studies of MMP3 [18] found out that the active site pocket next to the Zn vacant coordination site is too small to allow coordination of both a water and the substrate. However, in another QM based study where the possible coordination environment of the catalytic Zn ion was thoroughly analyzed, it was concluded that the most likely Zn coordination in the active enzyme involves two water molecules [19]. Given the numerous possibilities, regarding the zinc coordination, the

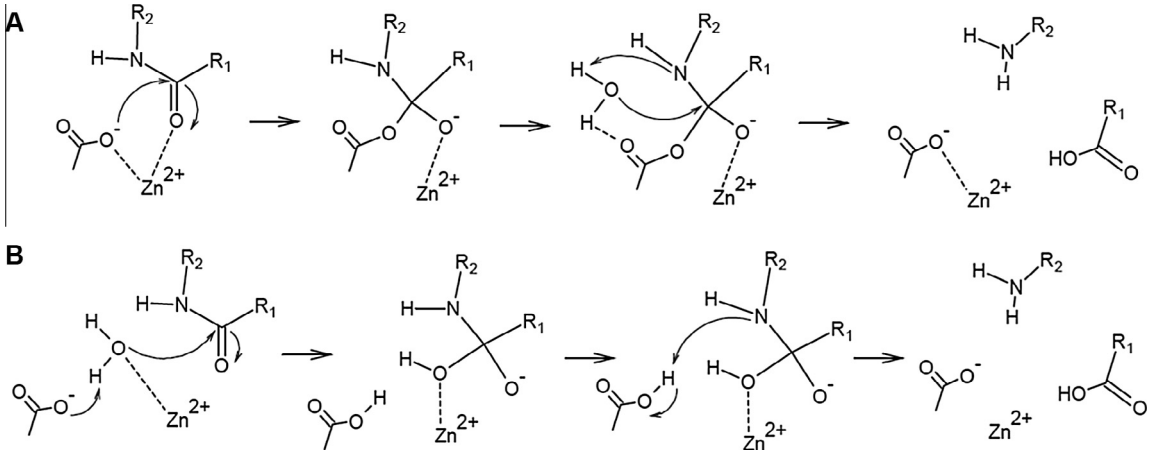

Fig. 1. Proposed reaction mechanisms of MMP3 proteolysis by (A) glutamate nucleophilic attack and (B) water nucleophilic attack.

water participation and the reaction mechanism, it is clear that a complete picture of the MMPs reaction mechanism is still missing. In this context, the main goal of our work is to study the MMP3 reaction mechanism, in order to test the different possibilities using state of the art DFT based QM/MM methods. Our results show that the reaction proceeds with a much lower barrier when a water molecule acts as a nucleophile toward the scissile peptide bond, and without substrate polarization, the reaction barrier is comparable to the barrier of the uncatalyzed reaction. Furthermore, it is shown that changes in the zinc coordination state prior to the reaction are crucial to achieve the described reactant configuration.

Methods

Starting structures and simulation parameters

Starting structures for the MMP substrate complex were derived from the pdb deposited structure pdbid 1M1W consisting of a monomer of active MMP3 with the bound peptide substrate GPLATCVP, the two Zn ions, and three Ca ions. The structural Zn coordination was tetrahedral with residues His201, His205, His211 and Glu202 as the coordinating residues. For the catalytic Zn several coordination patters were studied, tetrahedral coordination states consisting of three Histidines: His201, His205, His211, plus either the peptide substrate carbonyl (i.e. the carbonyl of the C–N scissile bond), the catalytic Glu202, or a water molecule. Additionally, trigonal bipiramidal Zn coordination states were modeled (i.e. with five ligands) consisting of the same three histidines, the substrate peptide carbonyl and either catalytic glutamate residue or a water molecule. All the different coordination stated of the catalytic zinc where built in-silico.

All classical simulations were performed by using the PMEMD module of the Amber10 package [20], with the Amber99SB force field parameters [21] for all residues, except the Zn and its coordination environment parameters which were specially determined and tested for each coordination type. The starting structures were immersed in a pre-equilibrated octahedral box of TIP3P [22] water molecules. SHAKE [23] was used to keep bonds involving hydrogen atoms at their equilibrium lengths, which allowed a 2-fs time step to be employed for the integration of Newton's equations. All simulations were performed at 1 atm and 300 K, and these conditions were maintained with the Berendsen barostat and thermostat [24], respectively. Periodic boundary conditions and Ewald sums [25] (grid spacing of 1 Å) were used to treat long range electrostatic interactions, and a 12 Å cutoff was used for computing direct interactions. After short 5 ns long MD simulations, used to allow the protein substrate structure to relax, and visual verification of a stable active site structure, the systems were slowly cooled to 0 K to obtain the initial structures for the QM/MM simulations.

QM/MM simulations

All optimizations were performed with a conjugate gradient algorithm, at the DFT level by using the SIESTA code [26] with QM/MM HYBRID implementation [27]. The quantum and the Molecular Mechanics subsystems are combined through a hybrid Hamiltonian introducing a modification of the Hartree potential and a QM/MM coupling term. The protein (or classical) environment around the active site affects the electronic density in a self-consistent fashion due to the addition of the classical point charge potential to the Hartree potential. The coupling term has two main contributions representing the electrostatic interaction between the electrons and nuclei, defining the QM charge density with the classical point charge and an additional term corresponding to the van der Waals interactions between the atoms in the quantum and classical regions through a 6–12 Lennard–Jones potential. For all atoms, basis sets of double zeta plus polarization quality were employed with cutoff and energy shift values of 150 Ry and 25 meV. All calculations were performed using the generalized gradient approximation functional proposed by Perdew, Burke, and Ernzerhof (PBE) [28]. Only residues located within 10 Å from the zinc reactive center were allowed to move freely in the QM/MM runs. The interface between the QM and MM portions of the system was treated with the scaled position link atom method (SPLAM). The SIESTA code showed excellent performance for medium-sized and large systems, and was proven to be appropriate for biomolecules [29,30]. For all systems the spin-unrestricted approximation was used, unless otherwise stated. In MMP3, the QM subsystem included the zinc atom the imidazole group of three His (H201, H205, H211), coordinating the zinc, a water molecule, a Glu carboxylate sidechain (E202) and the Ala-Thr-Leu portion of the natural substrate peptide where the scissile bond is located. To test the Glu-mediated mechanism, the QM system was the same, but without the water molecule. The rest of the protein unit and the water molecules were treated classically.

Determination of the reaction energy profiles

Since obtaining accurate free energy profiles requires extensive sampling, which is computationally very expensive and difficult to achieve at the DFT QM/MM level, we resorted to computing potential energy profiles by using restrained energy minimizations along the reaction path that connects reactant and product states. For this approach, an additional term, $V(n) = k(n - n_0)^2$, was added to the potential energy, where k is an adjustable force constant (set to be 200 kcal/mol in this study) and n_0 is a reference value, which was varied stepwise with an interval of 0.1 Å, along the reaction coordinate. By variation of n_0, the system is forced to follow the energy minimum reaction path along the given coordinate n. To avoid possible hysteresis problems in the reaction coordinate scans due to accidental changes in the MM part of the system, a distance cutoff of 10 Å from the QMMM region was used, which only allows MM atoms that are 10 Å away from any atom in the QM/MM to move during the reaction coordinate scan. By following this choice, 90% of the atoms in the protein are unconstrained. This method has been widely used in several works [27,30,32] and has been proven to successfully avoid the mentioned problem.

Method testing and Zn coordination parameter development

In order to determine and test the parameters for zinc and its coordination environment, the standard protocol for determination of classical force field parameters was used. Briefly, for each coordination type of zinc, model system calculations consisting for example, in a zinc plus three coordinated imidazol groups (representing histidine side chains) and either, an acetic acid (Glu side chain), a water, or a N-methyl acetamide (peptide bond) were performed in vacuum. Vacuum calculations were performed with the Gaussian program [31], using 6-31G* basis sets for hydrogen, carbon, nitrogen, oxygen and a LanL2DZ basis for the zinc atom and both B3LYP and HF methods. For each case, the partial atomic charges were determined using the RESP formalism, carefully analyzed and assigned for each coordination type. The van der Waals parameters were taken from Amber force field. All bonded parameters except those involving the zinc ion, were those corresponding to the same residue but uncoordinated. Bonded parameters equilibrium values for zinc were assigned based on the optimized structures in vacuum, while force constants were derived from frequency calculations or assigned based on

similarity with existing parameters in the amber force field. All these parameters are available under request. This methodology has been thoroughly tested by our group to develop metalloprotein parameters from several different cases including, iron [30], copper [32] and Mn [33]. The performance of the classical parameters was determined by performing short 5 ns MD simulations for the different coordination systems and analyzing the stability of the active site in comparison with the available crystal structures.

The effects of the Exchange Correlation functional and code were shortly analyzed, comparing the structural and energetic results for the model systems obtained with B3LYP-Gaussian [31] and PBE–SIESTA [26]. The singlet and triplet multiplicities of the whole system were tested, but the system showed very little sensibility to the spin state. For this reason, only the singlet results are presented. The results (data not shown) shows that both methods yield very similar optimized structures (up to 0.001 Å) and the difference in Zn bonding energy is about 10% , which is expected when comparing B3LYP and PBE functionals.

Results and discussion

QMMM optimization of the starting structures

In order to test the different possibilities proposed for the MMP reaction mechanism, a short 5 ns MD simulation was carried out from a PDB file template, obtained from docking studies of the model natural substrate to the MMP3 X-ray structure [18]. The simulation was made with a structure containing a water molecule in the active site and another that did not have the conserved water coordinated to zinc, in order to test the water-mediated and anhydride mechanisms. Since the active site is very tight to accommodate the usually proposed zinc coordination sphere, another MD simulation was made restraining the conserved water and the substrate carbonyl group close to zinc. This way, the influence of substrate polarization in the water-mediated mechanism could also be tested separately. The obtained results for the reactant geometries are consistent with a tetrahedrally coordinated zinc atom, usually observed in zinc proteases. When the water is absent, there is more room for the peptide substrate to access the active site to complete the coordination environment, with the oxygen atom 2.2 Å away from the catalytic zinc atom. When the conserved water molecule is present, it coordinates to zinc, with the oxygen atom at a distance of 2 Å from zinc, and one of the water hydrogen atoms gets closer to E202 carboxylate side chain, stretching the water O–H bond to 1.3 Å in the reactant state, which is also consistent with the observation that zinc proteases usually facilitate water deprotonation by lowering its pK_a. However, this was only observed when the substrate carbonyl group was close enough to coordinate to zinc, and this coordination controls the degree of water deprotonation. The QM/MM optimization of the MMP3 with the catalytic water yielded mainly two types of coordination: (i) the zinc atom coordinated to three histidines and one water molecule and (ii) the zinc atom coordinated to two histidines, one water molecule and the substrate carbonyl group. Although the pseudo-pentacoordination cannot be ruled out, it was not observed in the resulting QM/MM optimized configurations. Nevertheless, the observed classes of conformers would in principle enable the study of three different mechanisms: (i) the direct attack of the glutamate to the scissile peptide bond, forming the anhydride intermediate, and subsequent hydrolysis of the intermediate; (ii) water nucleophilic attack, with acid–base catalysis promoted by the glutamate side chain, without carbonyl substrate polarization by the catalytic zinc and (iii) same as (ii), but with simultaneous carbonyl substrate polarization, and therefore, the three mechanisms were investigated in the following sessions.

The geometrical parameters highlighted in Table 1 describe the main differences in the geometries and their relevance in the chosen reaction paths: The only possibility for simultaneous water and peptide substrate coordination is the detachment of one of the histidine nitrogens from the zinc atom, and the system remains in a tetrahedral coordination to zinc, and the penta-coordination was not observed. This last structure with simultaneous coordination to water and substrate also yielded the reaction mechanism with the lowest barrier, as will be discussed in the next sections.

Nucleophilic attack by water: the acid–base catalyzed pathway

In order to explore all the possibilities suggested by the QMMM optimized reactant structures, two possibilities for water nucleophilic attack were considered: the nucleophilic water attack with zinc polarizing just the attacking water molecule and the same mechanism, with zinc polarizing the water and the carbonyl substrate simultaneously (see Fig. 2).

Zn^{2+} assisted simultaneous substrate/water polarization

In order to simulate the hydrolysis reaction with simultaneous coordination of carbonyl substrate and water to zinc, the third reactant structure (see Fig. 4) was used as the reactant structure. In the relevant QM/MM optimized reactant geometry, it can be seen that two zinc histidine bonds remain by a distance of 2.0 A from the zinc atom, and the third one is displaced to 2.4 Å, while the distance from zinc to the water oxygen and zinc to substrate oxygen in the scissile peptide bond is around 3.2 Å. In this configuration, the glutamate is closer to the nitrogen of the peptide bond, and with the O–H bond in water already stretched to 1.32 Å. The d($C_{pep}N_{pep}$)–d($C_{pep}O_{wat}$) coordinate was used as the reaction coordinate to describe the potential energy surface (PES). As long as the C–O bond got gradually shorter, the displaced histidine nitrogen slowly moved close to the zinc atom again. In the former reaction mechanism proposed, the water could not approach the scissile peptide bond due to a strong hydrogen bond between the attacking water and an N–H group from a neighboring peptide bond in the substrate, between Thr5 and Cys6. However, the displaced histidine supplied the H-bond donor group for this role, while water was free to attack the peptide bond and donate the proton to the leaving group in the peptide bond being broken. Also noteworthy is that there was a second water molecule in the structure coordinating the carbonyl oxygen atom of the scissile peptide bond, as observed in previous studies [16], and it is claimed to supply extra electronic polarization to this group. Also, no tetrahedral intermediate was detected in the potential energy surface. The reaction proceeds with a computed barrier of

Table 1
Comparison among main geometrical parameters describing zinc coordination in each conformers from QM/MM geometry optimization. Structure A: zinc coordination to 3 histidines and the peptide substrate (without water); structure B zinc coordination to 3 histidines and 1 water molecule; structure C: zinc coordination to 2 histidines, 1 water molecule and the peptide substrate.

Geometrical parameter	Structure A	Structure B	Structure C
d Zn–N_{His1}	2.00	2.03	2.07
d Zn–N_{His2}	2.02	2.03	2.10
d Zn–N_{His3}	2.03	2.08	2.37
d Zn–O_{glu}	4.00	3.52	3.59
d Zn–O_{wat}	–	2.01	2.01
d Zn–O_{pep}	2.05	5.69	3.17
∠ N_{His1}–Zn–O_{pep}	110.95	108.37	117.75
∠ N_{His2}–Zn–O_{pep}	118.66	116.53	126.24
∠ N_{His3}–Zn–O_{pep}	101.88	104.64	144.71
∠ N_{His1}–Zn–O_{wat}	–	129.06	100.97
∠ N_{His2}–Zn–O_{wat}	–	106.73	117.97
∠ N_{His3}–Zn–O_{wat}	–	95.46	61.22

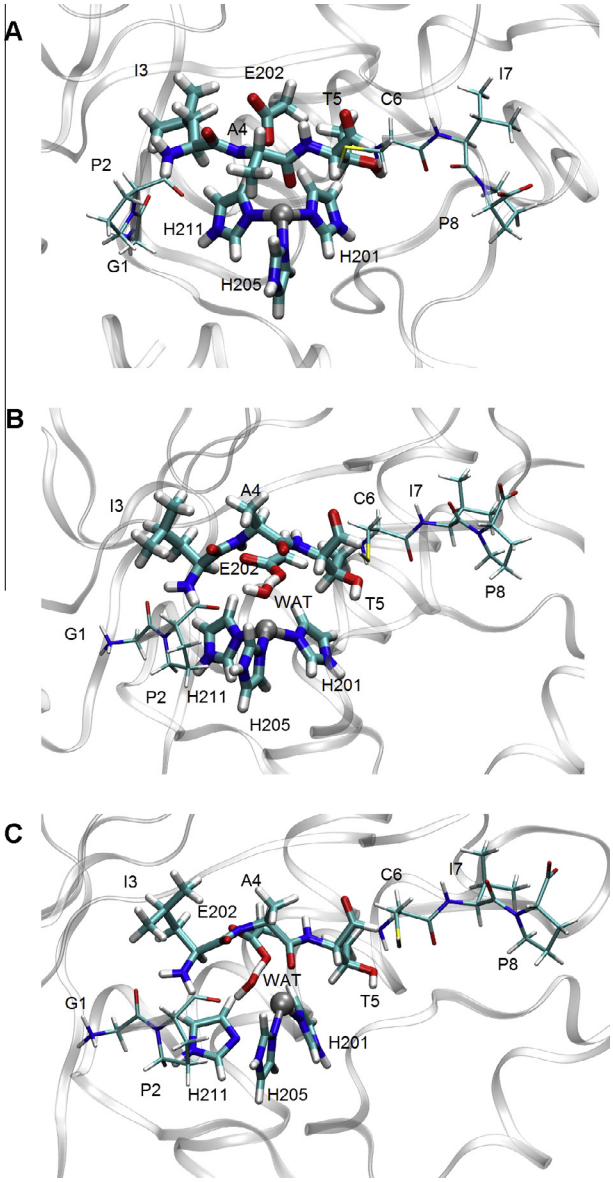

Fig. 2. QM/MM optimized geometry of the reactant complex of MMP3 and its natural substrate, without the active site conserved water molecule (A), the same complex, including the active site conserved water molecule, where only water is coordinated to zinc (B) and the same complex, including the active site conserved water molecule, where water and substrate are coordinated to zinc (C) The QM region is highlighted by thicker chemical bonds.

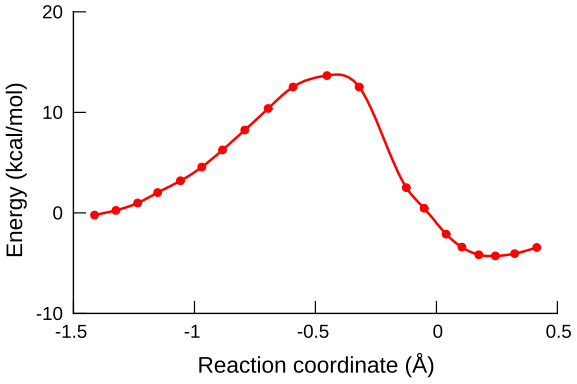

Fig. 3. Potential energy surface of MMP water attack reaction mechanism, using the $d(C_{pep}–N_{pep})–d(C_{pep}–O_{wat})$ difference as the reaction coordinate.

14.8 kcal/mol, with respect to the reactant minimum in the potential energy surface, in the direction of the final products.

By associating the Figs. 4 and 5, the evolution of the key distances over the reaction can be correlated with the main changes in energy, in the potential energy surface obtained in Fig. 4. In the course of reaction, the other two histidines are not depicted, since the distance between their epsilon nitrogen and the zinc atom remains unchanged, around 2 Å. As the restrained geometry optimization progresses, the third histidine slowly returns to the coordination sphere around zinc, which can be seen in the Zn–N_{his} distance in Fig. 4. The zinc atom remains tetra-coordinated in a tetrahedral geometry, with three histidines and one water molecule, and the oxygen from substrate carbonyl slowly approaches the zinc atom in the course of the reaction, as can be verified for the Zn–O_{wat} and Zn–O_{pep} distances. The third histidine keeps a little far from zinc, compared to the other histidines. Another important moment is depicted, when the water hydrogen is partially transferred to the peptide nitrogen, when a sharp drop in the $N_{pep}–H_{wat}$ distance from 2.3 Å to around 1.6 Å is observed, while the $O_{wat}–H_{wat}$ distance also has a sharp increase to 2.4 Å. These events correspond to the drop in energy, leading to the product, in the potential energy surface. From this point, the $C_{pep}–N_{pep}$ increases more notably, denoting the start of the $C_{pep}–N_{pep}$ bond break. The $C_{pep}–N_{pep}$ then gradually increases, from around 1.38 Å until it reaches the distance 1.76 Å in the geometry optimization of the potential energy surface. The decisive event which determines the end of the reaction happens where the water hydrogen is completely transferred to the amine free nitrogen, with another sharp drop in the $N_{pep}–H_{wat}$ distance, reaching the value of around 1.10 Å, and at the very same time the $N_{pep}–H_{wat}$ drops, the same decrease can be observed in the Zn–N_{his} distance, from 2.81 Å to 2.23 Å, and also the Zn–O_{wat} distance starts to increase. This can be seen as the final rearrangement of the zinc coordination environment in the catalytic site, leading to the regeneration of the reactant state, and it is follows by the major drop in energy in the PES. The $C_{pep}–O_{wat}$ distance no longer decreases significantly, also denoting the formation of the free carboxylic acid.

The Mulliken charge of key groups involved in catalysis is also analyzed along the reaction coordinate. The zinc atom charge changes from +0.88 e to +0.81 e. At the same time, the oxygen atom from the attacking water varies from −0.35 e to −0.25 e during the

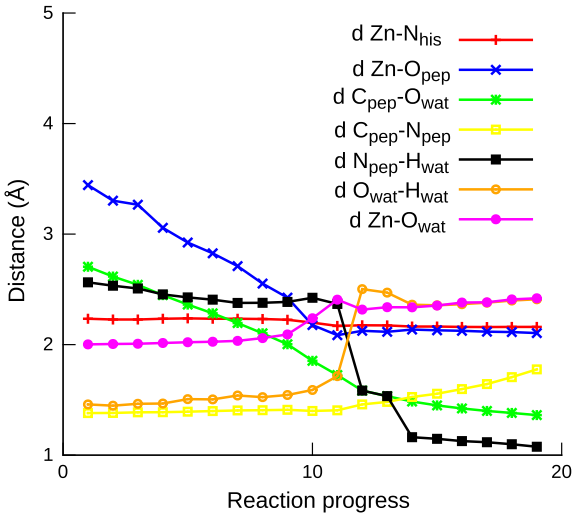

Fig. 4. Evolution of the key distances along the geometry optimization steps, identified as the reaction progress, corresponding to the reaction coordinate in Fig. 3.

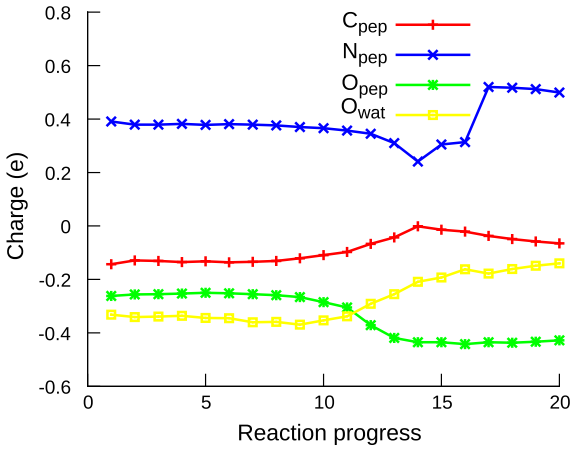

Fig. 5. Evolution of the Mulliken charges of key atoms along the geometry optimization steps, identified as the reaction progress, corresponding to the reaction coordinate in Fig. 3.

nucleophilic attack step, suggesting that a nucleophilic hydroxyl-like species is already formed before the approach of water to the substrate peptide bond. Shortly after the formation of the tetrahedral intermediate, when glutamate starts to transfer the abstracted water proton to the nitrogen leaving group, the other water proton becomes shared between the carboxylic acid product and the glutamate side chain, yielding a charge of +0.06 e. When the proton is completely transferred, and the reaction is complete, the glutamate strongly attracts the second water proton, resulting in the final free carboxylic acid product, with a charge of −0.21 e. During the same net charge reduction in zinc, the substrate carbonyl oxygen charge also changes from −0.29 e to −0.46 e in the water attack step. When the proton is transferred, the charge of the water oxygen attains the value of −0.28 e, and thus, at this stage, this oxygen atom leaves the zinc coordination sphere.

All these findings support a concerted hydrolysis reaction mechanism, where the first step is the water nucleophilic attack and deprotonation by the glutamate residue, leading to a gem-diol transition state, followed by the immediate glutamate proton transfer to the amine of the scissile peptide bond, with partial detachment of a histidine residue in the beginning of the reaction (see Fig. 6).

Apparently, the event controlling the general progress of the reaction is the coordination of the carbonyl substrate to zinc. The steric repulsion in the active site keeps one of the histidines 2.28 Å away from zinc, but in the course of the reaction, the same histidine helps to slowly destabilize the coordination between the water oxygen and zinc, and this is when the carbonyl oxygen can approach the zinc. When the water is bonded to the final product, it becomes hydrogen bonded to the glutamate, since the other water proton is already transferred to the amine. When another water molecule from the solvent replaces the carboxylic group of the product, the system is back to the initial state. In order to confirm this mechanism as the lowest barrier mechanism, the two other possible reaction mechanisms mentioned in the end of the previous section were tested.

Zn^{2+} assisted water polarization

In this section, we consider the nucleophilic attack performed by the oxygen in a conserved water molecule, in the active site, without substrate polarization by zinc atom. In the first QM/MM minimum energy structure, the water oxygen is the fourth ligand in zinc coordination sphere, and it is between the zinc atom and the peptide bond to be cleaved. The water approaches the peptide bond form the side, toward the carbonyl carbon. In the equilibrium structure, the oxygen is 2.01 Å away from the zinc, and one of the hydrogens is already partially detached from the water and being shared with the ionized glutamate side chain, with the corresponding hydrogen 1.13 Å away from water oxygen and 1.34 Å away from glutamate carboxyl oxygen. In this case, glutamate acts only as a base, deprotonating water and generating the hydroxide group to attack the peptide bond. In this structure, a penta-coordinated structure could not fit in the MMP pocket and carbonyl oxygen from the substrate is driven away from zinc, with a 5.69 Å initial distance. It is argued that zinc helps in lowering water p*K* and facilitate deprotonation, which converts water in a more powerful nucleophile, but the balance between steric repulsion and electrostatic attraction of key atoms in the active site is very delicate.

Several reaction coordinates were tested, and all yielded similar profiles. The results of the first step will be again presented in terms of the $d(C_{pep}O_{pep})$–$d(C_{pep}N_{pep})$ reaction coordinate. The observed barrier for water attack was 38 kcal/mol and a tetrahedral intermediate could be identified in the potential energy surface (see Fig. 7). In the intermediate, it can be seen that the C–N bond is almost broken, showing a C–N distance of 1.57 Å, and the water proton is already being shared between the glutamate and the amine leaving group, changing suddenly from a O–H distance of 1.73 Å in the TS to 2.51 Å in the following optimization step. The second step was simulated using $d(C_{pep}$–$O_{wat})$ coordinate, and it yielded a small barrier of 5 kcal/mol, leading to the final product and the glutamate regenerated to the ionized state. The barrier found is too high for an enzyme catalyzed reaction. The possible explanation is that when the water coordination is privileged, the hydroxyl species is formed too soon, and becomes strongly attached to the zinc atom. The simultaneous substrate polarization would help, not only to stabilize the substrate peptide carbon in an electron deficient configuration, but also, weaken the zinc–water bond. It can be seen that the coordinate abruptly changes in the TS, when suddenly the water hydrogen is transferred to the amine leaving group.

Glutamate nucleophilic attack: the anhydride reaction mechanism

To test the anhydride reaction mechanism, the QM region in question comprises the zinc atom, three coordinating histidines and three residues from the substrate to be hydrolyzed. The chosen reaction coordinate was the distance between one of the oxygen atoms from the catalytic glutamate residue to the carbon atom in the substrate, in the scissile peptide bond, minus the distance of the same carbon atom to the nitrogen atom in the peptide bond, that is, the $d(O_{Glu}C_{pep})$–$d(C_{pep}N_{pep})$ distance. The glutamate is considered as ionized, so the entire QM system comprised $a + 1$ charge.

In the reactant configuration, the distance between substrate carbon and glutamate oxygen was initially 3.06 Å, while at the same time, the distance of the substrate oxygen to the zinc atom is 2.06 Å. In the restrained geometry optimization, during the shortening of the C–O bond to 1.40 Å, as expected, the C–N peptide bond got longer, around 1.87 Å but the barrier increased continually, so we observed no stable anhydride intermediate formed in the reaction. It can also be seen that the glutamate keeps close to the zinc due to strong electrostatic attraction, and although the C–N bond reaches a high value, there is no water nearby to act as an acid and donate the proton to the amine leaving group. By doing a Mulliken charge analysis, it can be seen that glutamate transfer its charge entirely to the elements involved in the peptide bond (namely, the carbon, oxygen and nitrogen), and that zinc really plays a role of polarizing the environment (specially the carbonyl bond of the scissile peptide bond), rather than acting as an electron sink, since its charge remains almost unchanged during the reaction. To ensure no intermediate was formed, the reoptimization from the last structure obtained in the energy

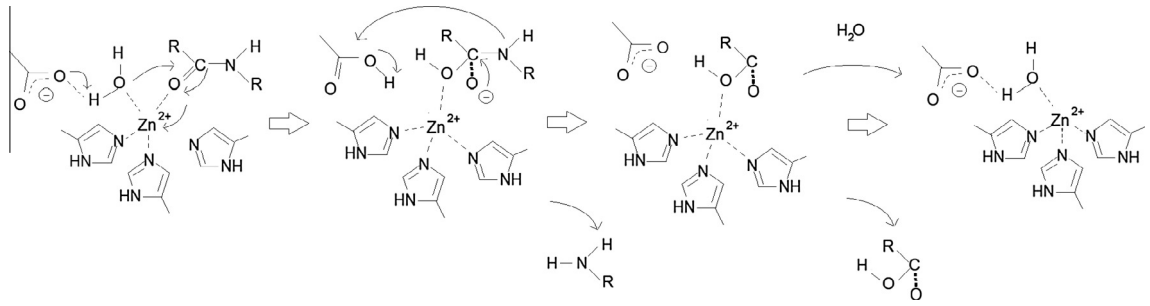

Fig. 6. Proposed reaction mechanism where acid–base catalysis is the most likely reaction, with a partial detachment of one of the histidine residues from zinc, in the early stages of the reaction.

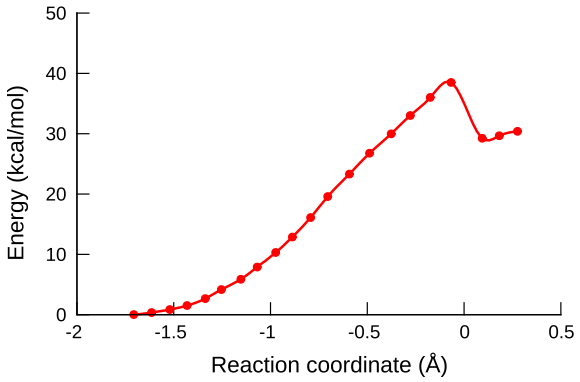

Fig. 7. Potential energy surface of the first step of MMP water attack reaction mechanism without substrate polarization, using $d(C_{pep}N_{pep})$–$d(C_{pep}O_{wat})$ as a reaction coordinate.

profile was attempted, and the system returned to the reactant configuration. Therefore, no stable products were observed and seems more likely that, at least one water molecule participates in the early stages of the reaction.

Conclusions

In this paper, a computer simulation investigation of the MMP3 catalytic mechanism is presented, highlighting the role of the zinc ion, the conserved water molecule and the glutamate in the reaction mechanism. The barriers found agreed with previous studies of other zinc enzymes, and the glutamate direct attack seems to be not feasible. However, the main important event in the beginning of the catalytic cycle is the substrate polarization, along with the formation of the hydroxide ion. Moreover, there is no room in the catalytic active site for the water and the substrate peptide bond at the same time in a penta-coordination arrangement, and one of the histidine residues moves out of zinc coordination sphere upon substrate binding. Previous studies of molecular dynamics [18] on MMP3 demonstrate that the pocket in active site does not have space for water and the substrate carbonyl at the same time it keeps three histidines coordinated to zinc, so if the natural substrate is bound to the enzyme, one of the above ligands is displaced from the zinc atom. These results led the authors to propose the glutamate-mediated mechanism, since zinc could not polarize the water molecule and the substrate at the same time. In the same study, a possible protein substrate structure of MMP3 was generated and deposited in the PDB with code 1M1W. However, for the results in this work, it is unlikely that the anhydride route will produce a reactive pathway to MMP3.

In order to evaluate the contribution of the enzyme to the catalysis, the hydrolysis reaction was also simulated in the absence of the MM region of the enzyme. The system comprised the same QM region considered in the QM/MM simulations of the water attack reaction mechanism. The optimized reactant structure showed essentially the same features of the water attack mechanism. The barrier was much higher, though: around 34 kcal/mol. The histidine failed to return to the initial coordination state, and remained far from zinc in the end of the reaction. Since the active site is very exposed to the solvent, and there are no other polar residues around the active site, the difference could be attributed to the lack of specific interactions of the solvent with the substrate and active site, in the geometry by which the substrate binds to the enzyme. It has been shown recently that solvent dynamics can exert significant control in MMP reaction kinetics [34].

In the proposed route of this work, the hydrogen for the amine protonation comes from the conserved water molecule in the active site, and the glutamate helps transferring a proton, from the water to the nitrogen of the peptide bond. Specific interactions of the partially displaced histidine with atoms from the substrate leave the catalytic glutamate free and flexible enough to promote acid–base catalysis. More recent studies [17] of the reaction catalyzed by MMP-2 with its natural substrate, by QM/MM and Poisson–Boltzmann methods pointed out that if the substrate is too long, the geometric restrictions usually applied in QM/MM artificially restrict some degrees of freedom of the substrate, preventing it from being protonated, or even cleaved, leading to serious artifacts in the potential energy surface. For example, a recent QM/MM DFT computer simulation study of CPA with the natural substrate of the enzyme found a 14.6 kcal/mol barrier for water-mediated attack [15]. However in this particular work, it was pointed out that abrupt changes can happen in the energy optimization along the path, depending on the chosen reaction coordinate. Also it is not confirmed if the tetrahedral intermediate is correct due to the simplified description of the substrate.

In previous work [16], a DFT-B3LYP QM/MM study of the MMP3 enzyme yielded a single step reaction consisting of a water nucleophilic attack with a barrier of 13.1 kcal/mol for an acetamide model substrate. It is also postulated that a second water molecule is important in polarizing the substrate, since MMP3 lacks the usual sidechains in other zinc proteases and there is an additional stabilization of the transition state by 5 kcal/mol. It was also pointed out that more water molecules could participate in the reaction. One limitation pointed out by the authors is that since it is a model substrate, it is much more flexible than the natural substrate, and the barrier for the protonation of the amine leaving group could be underestimated. In the mechanism proposed in this paper, in the lowest-barrier mechanism, the second conserved water is also observed, and indeed, it aids in substrate polarization, lowering the barrier for nucleophilic attack. The penta-coordination proposed in this study though, could not be observed in the present work, probably due to the difference in the steric hindrance when considering a model substrate, compared to the real substrate, and yet, the both studies compare pretty well to experimental data.

In summary, this is the first work with considers also the role of the entire model substrate in the simulation of the reaction path for MMP3. The results in present work, thus favor the water-mediated peptide hydrolysis, with a new role for one of the histidines in the coordination environment, which can provide new strategies for designing specific zinc-metalloprotein inhibitors with therapeutically useful applications.

Acknowledgements

The authors would like to thank CNPq for the financial support and the Institute of Physics of University of São Paulo, particularly the SAMPA group, and the Institute of Chemistry of São Paulo State University in Araraquara, particularly the Nanobionics research group – UNESP Araraquara, Brazil for the computational resources.

Appendix A. Supplementary material

Supplementary data associated with this article can be found, in the online version, at http://dx.doi.org/10.1016/j.molstruc.2015.02.079.

References

[1] N. Borkakoti, Prog. Biophys. Mol. Biol. 70 (1998) 73–94.
[2] H.G. Welgus, Agents Actions Suppl. 35 (1991) 61–67.
[3] M.D. Sternlicht, Z. Werb, Annu. Rev. Cell Dev. Biol. 17 (2001) 463–516.
[4] H. Nagase, J.F. Woessner, J. Biol. Chem. 274 (1999) 21491–21494.
[5] M. Browner, Perspect. Drug Discovery Des. 2 (1995) 343–351.
[6] A.I. Marcy et al., Biochemistry 30 (1991) 6476–6483.
[7] L.P. Kotra et al., J. Am. Chem. Soc. 123 (2001) 3108–3113.
[8] M.F. Browner, W.W. Smith, A.L. Castelhano, Biochemistry 34 (1995) 6602–6610.
[9] N. Díaz, D. Suárez, Biochemistry 46 (2007) 8943–8952.
[10] I. Bertini et al., Angew. Chem. Int. Ed. 45 (2006) 7952–7955.
[11] D.W. Christianson, W.N. Lipscomb, Acc. Chem. Res. 22 (1989) 62–69.
[12] R. Breslow, D.L. Wernick, Proc. Natl. Acad. Sci. USA (1977) 1303–1307.
[13] D. Mustafi, M.W. Makinen, J. Biol. Chem. 269 (1994) 4587–4595.
[14] H.C. Lee, Y.H. Ko, S.B. Baek, D.H. Kim, Bioorg. Med. Chem. Lett. 8 (1998) 3379–3384.
[15] M.W.Y. Szeto, J.I. Mujika, J. Zurek, A.J. Mulholland, J.N. Harvey, J. Mol. Struct.: THEOCHEM 898 (2009) 106–114.
[16] V. Pelmenschikov, P.E.M. Siegbahn, Inorg. Chem. 41 (2002) 5659–5666.
[17] N. Díaz, D. Suárez, J. Phys. Chem. B 112 (2008) 8412–8424.
[18] S. Manzetti, D.R. McCulloch, A.C. Herington, D. van der Spoel, J. Comput.-Aided Mol. Des. 17 (2003) 551–565.
[19] N. Díaz, D. Suárez, T.L. Sordo, J. Phys. Chem. B 110 (2006) 24222–24230.
[20] D.A. Pearlman et al., Comput. Phys. Commun. 91 (1995) 1–41.
[21] V. Hornak et al., Proteins: Struct., Funct., Bioinform. 65 (2006) 712–725.
[22] W.L. Jorgensen, J. Chandrasekhar, J.D. Madura, R.W. Impey, M.L. Klein, J. Chem. Phys. 79 (1983) 926–935.
[23] J.-P. Ryckaert, G. Ciccotti, H.J.C. Berendsen, J. Comput. Phys. 23 (1977) 327–341.
[24] H.J.C. Berendsen, J.P.M. Postma, W.F. van Gunsteren, A. DiNola, J.R. Haak, J. Chem. Phys. 81 (1984) 3684–3690.
[25] T. Darden, D. York, L. Pedersen, J. Chem. Phys. 98 (1993) 10089–10092.
[26] M.S. José et al., J. Phys.: Condens. Matter 14 (2002) 2745.
[27] A. Crespo, M.A. Martí, D.A. Estrin, A.E. Roitberg, J. Am. Chem. Soc. 127 (2005) 6940–6941.
[28] J.P. Perdew, K. Burke, M. Ernzerhof, Phys. Rev. Lett. 77 (1996) 3865–3868.
[29] D.E. Bikiel et al., Phys. Chem. Chem. Phys. 8 (2006) 5611–5628.
[30] M.A. Martí, L. Capece, A. Crespo, F. Doctorovich, D.A. Estrin, J. Am. Chem. Soc. 127 (2005) 7721–7728.
[31] M.J. Frisch, et al., Gaussian 98, Revision A.11.4, 2002.
[32] A. Crespo, M.A. Martí, A.E. Roitberg, L.M. Amzel, D.o.A. Estrin, J. Am. Chem. Soc. 128 (2006) 12817–12828.
[33] D.M. Moreno et al., Arch. Biochem. Biophys. 507 (2011) 304–309.
[34] M. Grossman, B. Born, M. Heyden, D. Tworowski, G.B. Fields, I. Sagi, M. Havenith, Nat. Struct. Mol. Biol. 18 (2012) 1102–1108.